

## **Vibration Control of Stress Waveform Superposition in Millisecond Blasting**

\*Qing Li, \*\*Yaodong Xue\*, \*\*\*Di Zhang

\* School of Mechanics & Architecture Engineering, Faculty of Geotechnical Engineering,  
University of Mining & Technology (Beijing), Beijing 100083, China

\*\* School of Mechanics & Architecture Engineering, Faculty of Geotechnical Engineering,  
China University of Mining & Technology (Beijing), Beijing 100083, China  
(xuecumtb@163.com)

\*\*\*School of Civil Engineering, Guangzhou University, Guangzhou 510006, China

### **Abstract**

Based on the measured signals of single-hole blasting, this paper constructs the superposed stress waveform of blasting at different time delays by the linear superposition method, and studies the distribution of vibration velocity and energy. The results show that the maximum superposed vibration velocity was apparently reduced when the time delay lasted no longer than half the cycle of a waveform. Owing to the complexity of waveforms, a half-cycle superposed velocity may not be the minimum velocity of the synthetic wave. When  $T/2 < t < T$ , the superposed vibration velocity simultaneously increased and approximated the maximum vibration velocity. The total energy of the millisecond blasting was basically lower than that when the two holes were blasted simultaneously. The total energy of the single-hole waveform had a minimum value, and the energy ratio decreased faster when the time difference is in the range of half-cycle. The author also calculated the optimal time delay ranges of the three cases.

### **Key words**

Subway tunnel, Blasting vibration control, Wave superposition, Complete ensemble empirical mode decomposition (CEEMD), Energy distribution.

## 1. Introduction

During the drilling and blasting of urban subway construction, the blasting vibration must be strictly controlled due to the closeness of the excavation site to the ground. With electronic detonators, it is now possible to set precise time delays, achieve good rock crushing effect, and reduce the strength of blasting vibration. The key and difficult point of electronic blasting is to ascertain the relationship between the vibration strength and time delay.

The previous studies have predicted the vibration strength at different time delays and deduced the reasonable inter-hole time delay, using neural network method [1-4], numerical simulation[5-7] and wave superposition method [8-10]. Based on the single-hole blasting waveform measured in an actual subway tunnel, this paper constructs the superposed stress wave at different time delays by the linear superposition method, aiming to shed new light on actual tunnel blasting.

## 2. Methodology

### 2.1 Feasibility of single-hole wave superposition

The single-hole blasting waveform contains all the information of the blasting site, and lays the basis for deducing the theoretical waveform of vibration velocity in multi-hole blasting. According to Brune's research [11], the vibration velocity of multi-hole millisecond blasting can be expressed as [12]:

$$V = v_s \sum_{i=1}^n a_i \delta_i(t - t_i) \quad (1)$$

where  $v_s$  is the velocity waveform of single-hole blasting;  $V$  is the superposed waveform of multi-hole millisecond blasting;  $a_i$  is the amplitude ratio coefficient of any single-hole blasting with the waveform of  $v_s$ ;  $\delta_i$  is the blasting pulse function of different blasting holes.

In most of the existing studies, it is assumed that the vibration curve of multi-hole blasting can be linearly superposed by that of single-hole blasting, and that the imitation time, i.e. the time delay, can be precisely controlled. Hence, formula (1) is often simplified as:

$$V(t) = \sum_{i=1}^n v_i(t + \Delta t_i)$$

(2)

where  $\Delta t_i$  is the time delay between the  $i$ -th hole and its adjacent hole;  $v_i(t)$  is the vibration velocity waveform of the  $i$ -th hole blasting;  $V(t)$  is the waveform superposed by that of all holes. Since the electronic blasting obeys formula (2), the author applied the formula to analyse the superposition of single-hole blasting waveforms and the damping effect at different time delays.

## 2.2 Waveform Acquisition

The research object is a subway tunnel under construction. The roof of the tunnel is 23m beneath the ground. The soil layer and the rock layer are respectively 12m and 11m in thickness. Two subway lines are planned in the tunnel. The tunnel wall is 11.5-11.6m thick. The tunnel is constructed by the benching method with the sectional size of the upper bench of 6.4m×3.15m.

In total, three single-hole blasting waveforms of different blasting parameters were sampled from the upper bench. Two waveforms were selected from the ground perpendicular to the tunnel: one with 1.2kg of explosives and main frequency of 50Hz, and the other with 1.5kg of explosives and main frequency of 46Hz. The rest one waveform was collected from the adjacent tunnel with 1.5kg of explosives and main frequency of 135Hz. Figure 1 illustrates the three blasting vibration waveforms.

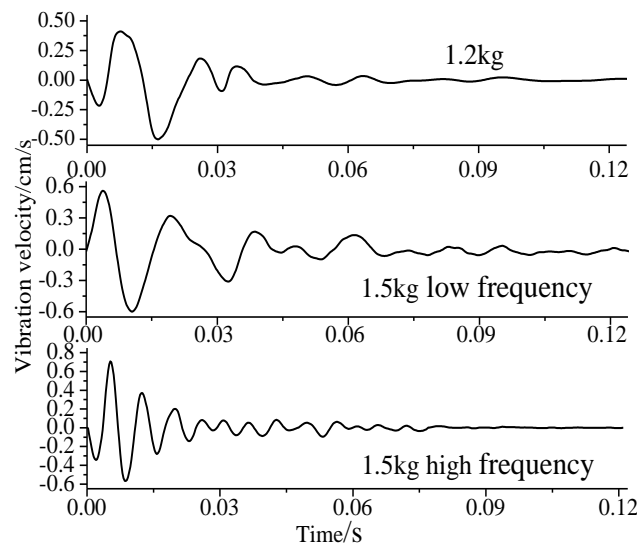


Fig.1. Three blasting vibration waveforms

As shown in Figure 1, the maximum vibration velocities of the waveform with 1.5kg of explosives, the waveform with 1.5kg of explosives, and the waveform collected from the adjacent tunnel are 0.499cm/s, 0.598cm/s and 0.707cm/s, respectively.

The tunnel is buried deeply in the ground. The vault is separated by thick layers of soil and rock from the surface. In the soft medium of soil, the stress wave velocity and high frequency components attenuate rapidly, and the main frequency remains at a low level. In the hard medium of rock, however, the attenuation of the stress wave velocity and high frequency components is relatively slow, and the main frequency remains at a high level. Under the same explosive quantity, the vibration velocity and main frequency in the rock layer are higher than the results measured on the ground.

## 2.3 Waveform Fitting

This research mainly focuses on the waveform superposition pattern of double-hole blasting at different time delays. In view of the numerous waveforms being superposed, the program was compiled in MATLAB, and the nonlinear fitting was conducted on the measured waveforms in reference to [13]:

$$f(t) = a_0 + \sum_{i=1}^8 a_i \cos(i\omega t) + \sum_{i=1}^8 b_i \sin(i\omega t) \quad (3)$$

where  $i$  is the goodness of fit;  $a_0$ ,  $a_i$  and  $b_i$  are the fitting coefficients the fitting coefficients.

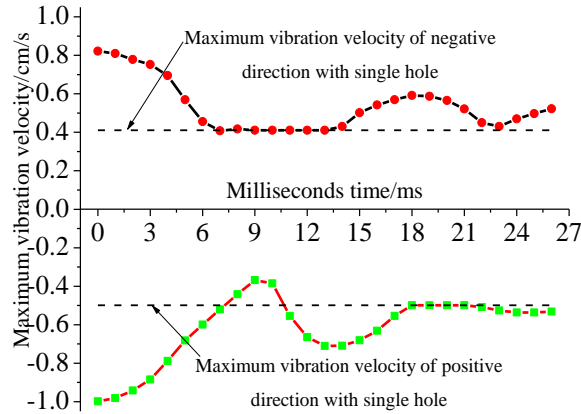
The fitting coefficient obtained from a single fitting function is relatively low, and the stress wave is often manual segmented with zero vibration speed as discontinuous points. Taking the single-hole blasting waveform with 1.2kg of explosives as an example, the double-hole wave superposition formula is constructed as follows:

$$V_{s1.2}(t) = \begin{cases} f_1(t) & t \leq \Delta t \\ f_1(t) + f_1(t - \Delta t) & \Delta t < t \leq t_1 \\ f_1(t - \Delta t) + f_2(t) & t_1 < t \leq t_1 + \Delta t \\ f_2(t) + f_2(t - \Delta t) & t_1 + \Delta t < t \leq t_2 \\ f_2(t - \Delta t) + f_3(t) & t_2 < t \leq t_2 + \Delta t \\ f_3(t) + f_3(t - \Delta t) & t_2 + \Delta t < t \leq t_{\max} \end{cases} \quad (4)$$

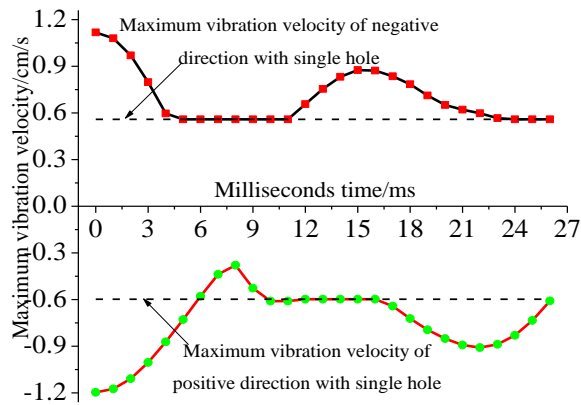
where  $\Delta t$  is the time difference;  $t_{\max}$  is the total waveform length. When  $\Delta t > t_1$ , the superposed waveform formula can be deduced according to formula (5). The superposed waveforms of the other two cases were deduced in a similar manner.

### 3. Effect of Time Delay on Vibration Velocity

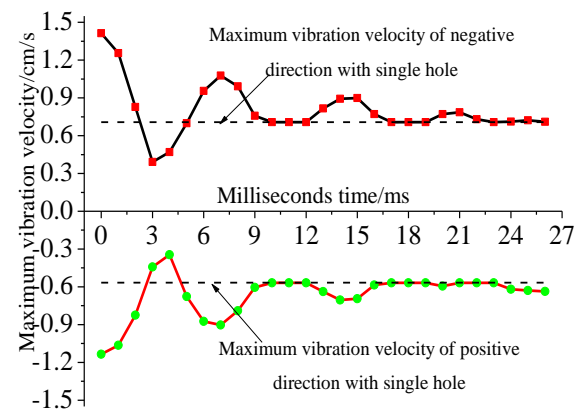
The single-hole blasting waveforms in Figure 1 were superposed at different time delays. The time difference  $\Delta t$  was set to 1ms for the iteration. Figure 2 shows the maximum waveform velocity in the positive and negative directions of the three cases. The total time difference was selected as  $\Delta t = 0-26$  ms.



(a) Signal hole blasting waveform with 1.2kg of explosives



(b) Signal hole blasting waveform with 1.5kg of explosives at low frequency



(c) Signal hole blasting waveform with 1.5kg of explosives at high frequency

Fig.2. The maximum superposed vibration velocities of double-hole blasting in both positive and negative directions of the three cases

In the three cases, the maximum vibration velocity of the double-hole blasting appeared at 0ms and 1ms. As shown in Figure 2(a), the superposed vibration velocity of the waveform with 1.2kg of explosives attenuated slowly at  $\Delta t=4\text{ms}$ , and declined almost linearly from 4ms to 7ms. After 7ms, the positive vibration velocity remained unchanged with an amplitude equivalent to the maximum positive vibration velocity of single-hole blasting, while the negative vibration velocity decreased after reaching the maximum single-hole blasting vibration velocity. At  $\Delta t=9\text{ms}$ , the negative vibration velocity arrived at the lowest point, and the maximum amplitude in both positive and negative directions were equal to or lower than the peak vibration velocity of single-hole blasting. Suffice it to say that the single-hole blasting with 1.2kg of explosives achieved continuous detonation when  $\Delta t$  fell in the range of 7-10ms. Any further increase in  $\Delta t$  would lead to gradual decline in the superposed vibration velocity. This is also the case in the low frequency and high frequency waveforms with 1.5kg of explosives. It is concluded that the time difference should not be widened blindly within a certain period of time delay, as the maximum vibration velocity would fluctuate cyclically with the change of time difference.

In Figure 2(b), the maximum superposed vibration velocity attenuated in a similar way with that of the case with 1.2kg of explosives. Of course, the attenuation rate was faster than that of the case with 1.2kg of explosives at small time differences. At  $\Delta t=4\text{ms}$ , the superposed velocity in the positive direction was reduced to the maximum positive velocity of single-hole blasting, which achieved initiation in  $\Delta t=6-11\text{ms}$ . This is because the quantity of explosives is positively correlated with the vibration velocity in the blasting zone. The vibration velocity attenuated exponentially with the increase in the blasting heart rate. The faster the vibration velocity, the faster the rate of attenuation. The velocity attenuation features of the two cases echo with the results of previous studies, and hold evidence to the feasibility of the linear superposition of waveforms.

According to Figure 2(c), the double-hole superposed velocity of the single-hole blasting waveform collected from the adjacent is much more complicated than that of the other cases. At small time differences, the superposed vibration velocity attenuated faster than the vibration velocity of single-hole blasting. At  $\Delta t=4-5\text{ms}$ , the superposed velocity in both the positive and negative directions stayed below than that of single-hole blasting but rebounded rapidly to the peak of  $1.08\text{cm/s}$  at  $\Delta t=7\text{ms}$ . This means the improper time difference of electronic detonators had pushed up the vibration intensity, adding to the difficulty in blasting vibration control.

Based on the attenuation patterns of the superposed velocities in the above three cases, it can be seen that the peak-valley superposed vibration was reduced when the time delay lasted no longer than half the cycle of a waveform; the superposed vibration velocity was lower than the maximum velocity of single-hole blasting. Owing to the complexity of waveforms, a half-cycle superposed velocity may not be the minimum velocity of the synthetic wave.

When  $T/2 < t < T$ , the superposed vibration velocity simultaneously increased and approximated the maximum vibration velocity. In light of this, the actual rational time delay should be applied to the engineering practice. If the same time difference is implemented in different scenarios, it is impossible to achieve the desired vibration or satisfactory rock crushing effect between the holes.

If the two holes are blasted simultaneously, the maximum vibration velocity of the superposed waveform and the attenuation rate  $r_v$  of the maximum vibration velocity can be obtained by formula (5).

where  $v_{max}$  is the maximum vibration velocity of the superposed waveform at simultaneous blasting;  $v$  is the maximum superposed velocity at varied time differences. Figure 3 displays the attenuation rates of the three cases calculated by formula (5).

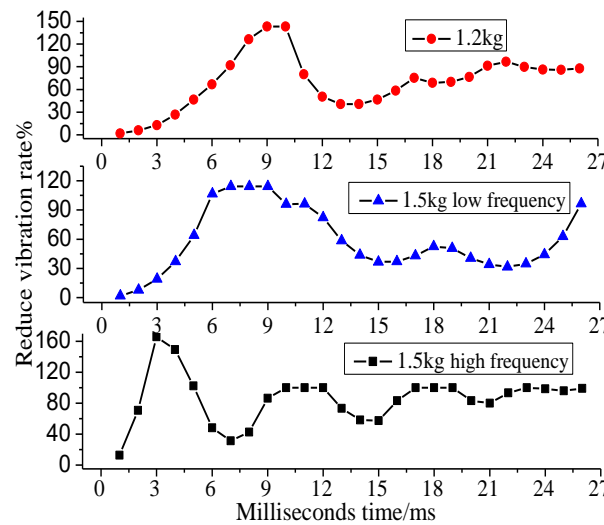


Fig.3. The attenuation rates of vibration velocities of the three cases at different time differences

It can be seen from Figure 3 that when the time difference approached the half cycle of the waveform, the attenuation rates of the three cases were over 100%, and the vibration velocities of the superposed waveforms were smaller than the maximum velocities of single-hole blasting. When the time difference exceeded the half cycle of the waveform, the attenuation rates started to

decrease, and the vibration velocities of cases 2 and 3 were merely 30%-50% at  $\Delta t=12-16\text{ms}$ . Hence, the anti-vibration effect of non-half cycle wave superposition is not obvious.

According to the theory of blasting wave superposition, the maximum degree of vibration reduction can be achieved via peak-valley superposition if two waveforms are only half a cycle long. Based on the main frequencies of the waveforms, the half cycles of the three cases were calculated as  $T_{1.2}=9.6\text{ms}$  (case 1),  $T_{1.5l}=10.6\text{ms}$  (case 2), and  $T_{1.5h}=3.7\text{ms}$  (case 3).

## 4. Energy Distribution Features of Superposed Waveforms

### 4.1 CEEMD Decomposition Principle

This section adopts the complete ensemble empirical mode decomposition (CEEMD) principle, which is the improved version of the popular method of empirical mode decomposition (EMD) [14].

$$\begin{cases} x_1^+(t) = x(t) + n_1(t) \\ x_1^-(t) = x(t) - n_1(t) \end{cases} \quad (6)$$

Through the treatment of  $x_1^+(t)$  and  $x_1^-(t)$  in the CEEMD, the resulting  $IMF_{1+}$  and  $IMF_{1-}$  can be combined into the following modal component:

$$IMF_1 = [IMF_{1+} + IMF_{1-}] / 2 \quad (7)$$

After the signal is decomposed, the instantaneous energy spectrum and the marginal spectrum of the signal are obtained according to formulas (8) and (9), respectively:

$$IE(t) = \int_{\omega} H^2(\omega, t) d\omega \quad (8)$$

$$ES(\omega) = \int_0^T H^2(\omega, t) dt \quad (9)$$

### 4.2 Effect of Time Difference on Vibration Energy



Single-hole blasting releases a fixed amount of energy. When the vibration waveform is superposed, the superposed energy peaks at 0ms, about twice the energy of single-hole blasting. With the increase in time difference, the superposed energy also changes. In this research, the superposed waveforms of the three cases were decomposed by the CEEMD to obtain the instantaneous energy is obtained of each IMF component according to formula (9). Then, the instantaneous energies of the superposed waveforms at different time delays were added up to get the total energy of the superposed waveform. To facilitate observation, all the energies were normalized: the double-hole superposed energy was set to 1 at 0ms, and the remaining energies were divided by the energy at 0ms. Figure 4 displays the superposed energies of the three cases at varied time differences.

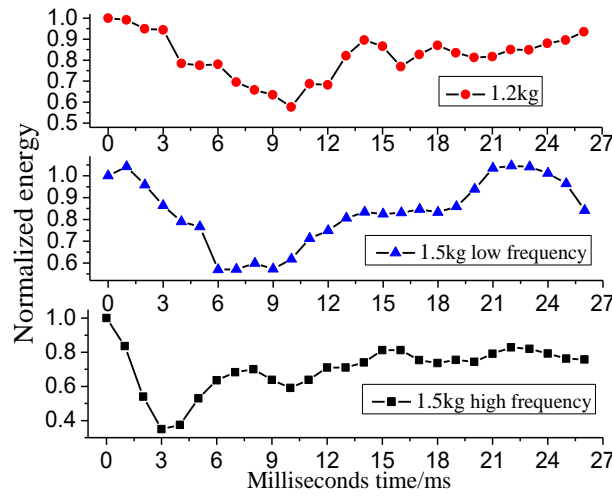


Fig.4. Variation of Normalized Energies of the Three Cases at Varied Time Differences

The relationship between instantaneous energy and velocity is expressed as:

$$V_{\Delta E} = \sqrt{2\Delta E_{\max}} \quad (10)$$

where  $V_{\Delta E}$  is the equivalent velocity;  $\Delta E_{\max}$  is the maximum instantaneous energy. It is clear that the vibration velocity is proportional to the instantaneous energy. When the instantaneous energy is added to the total energy, there is also a proportional relationship between the total energy and the vibration velocity. Hence, whenever the signal achieves the vibration velocity, the instantaneous energy should also reach the peak value, that is, the maximum total energy should climb up. The inverse is also true.

As shown in Figure 4, the total energy released by the blasting at different time delays was basically lower than the total energy of the detonation at the same time. The total energy reached the minimum value in the half cycle of the superposed signal. In other periods, the total energy dropped and grew gently across the three cases. At long time delays, the total energy gradually approached the superposed energy at 0ms. Meanwhile, the superposed energies of cases 1 and 2 were greater than the total energy of single-hole blasting. The above results show that it is impossible to achieve the single-hole blasting even if the half-cycle is adopted because of the overlap between the stress waves generated by different holes.

In view of the generally low natural frequency of ground buildings, the author analysed the energy distribution within 0-20Hz at varied time differences. After the CEEMD decomposition of the superposed signal, the marginal spectrum of the signal was obtained according to formula (9), and the proportion of energy in 0-20Hz to the total energy (energy ratio) was calculated. Whereas the blasting signal had a low frequency, the total frequency band was set to 250Hz. The energy ratios of the three cases are depicted in Figure 5.

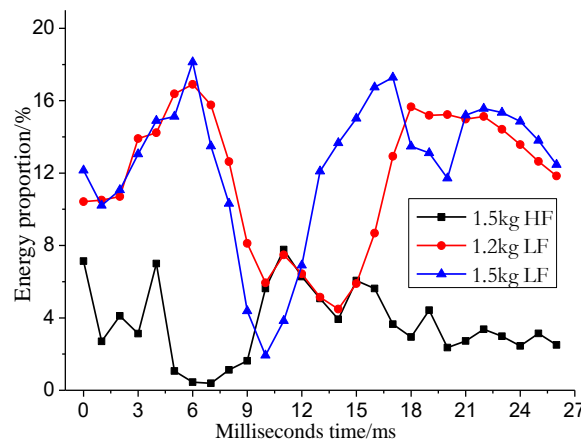


Fig.5. The proportion of the energy in 0-20Hz to the total energy of the three cases at varied time differences

Overall, case 3 had the smallest energy ratio, which peaked at 7.9% at 11ms. Cases 1 and 2 boasted relatively high energy ratios, where were maximized at 17.2% and 18.5%, respectively, at  $\Delta t=6$ ms. For case 3, the energy ratio increased rapidly at  $\Delta t=4$ ms, and remained low at  $\Delta t=5-9$ ms, indicating that the blasting had little disturbance on the buildings. For cases 1 and 2, the energy ratios declined sharply after the rapid rise in  $\Delta t=6-17$ ms. In the  $\Delta t=9-12$ ms, the energy ratios of the two cases were 8% and even less. This means the time difference in this period produces less vibration to the buildings. With further expansion of the time difference, the energy ratios of the

two cases maintained at a relatively high level. Hence, the time difference after 12ms should not be adopted.

The energy ratio is an important parameter for mitigating the negative effect of blasting on surface buildings. When the stress wave propagates to the ground, most of the high-frequency components are absorbed, and the signal frequency measured on the ground is relatively low. In the case of excessive low-frequency energy, the buildings may be destroyed even if the velocity does not exceed the standard. Apart from setting a rational time difference, the energy ratio should also be minimized to ensure the safety of the buildings.

To sum up, in the main vibration frequency of 45-55Hz, the best damping effect can be achieved by setting the time differences of cases 1, 2 and 3 at 9-11ms, 9-10ms and 9-10ms, respectively. In the main frequency of 135-145Hz, the time differences of the three cases should be set to 3ms, 5ms and 6ms, respectively.

## Conclusion

(1) The linear superposition method was relied on to construct the superposed stress waveforms at different time delays. It is concluded that the maximum superposed vibration velocity was apparently reduced when the time delay lasted no longer than half the cycle of a waveform. Owing to the complexity of waveforms, a half-cycle superposed velocity may not be the minimum velocity of the synthetic wave. When  $T/2 < t < T$ , the superposed vibration velocity simultaneously increased and approximated the maximum vibration velocity.

(2) The total energy of the millisecond blasting was basically lower than that when the two holes were blasted simultaneously. The total energy of the single-hole waveform at half-cycle and the near-time range had a minimum value, and the superposed energy was greater than that of the single-hole blasting energy. Meanwhile, the energy ratio decreased faster when the time difference is in the range of half-cycle. The author also calculated the optimal time delay ranges of the three cases.

(3) The rational time difference must fall in an interval, in which the blasting parameters are designed to improve the damping effect. In actual practice, the detonation time of the electronic detonator should be designed according to the vibration amplitude, the distance to the explosion centre and the energy distribution features of the protected structures.

## Acknowledgment

This paper was supported by “The National Natural Science Foundation of China (NO.51374212)”.

## References

1. G. Zhang, Y.W. Yang, Z.J. Liu, J. Wang, Prediction of blasting vibration velocity by BP neural network, 2014, *Applied Mechanics & Materials*, vol. 539, pp. 736-740.
2. M.T. Mohamed, Artificial neural network for prediction and control of blasting vibrations in Assiut (Egypt) limestone quarry, 2009, *International Journal of Rock Mechanics & Mining Sciences*, vol. 46, no. 2, pp. 426-431.
3. S. Lv, S. Lv., Applying BP neural network model to forecast peak velocity of blasting ground vibration, 2011, *Procedia Engineering*, vol. 26, pp. 257-263.
4. S. Roy, G.R. Adhikari, T.A. Renaldy, A.K. Jha, Development of multiple regression and neural network models for assessment of blasting dust at a large surface coal mine, 2011, *Journal of Environmental Science & Technology*, vol. 4, no. 3, pp. 284-301.
5. J.H. Yang, W.B. Lu, Q.H. Jiang, C. Yao, C. B. Zhou, Frequency comparison of blast-induced vibration per delay for the full-face millisecond delay blasting in underground opening excavation, 2016, *Tunnelling & Underground Space Technology*, vol. 51, pp. 189-201.
6. W. Lu, J. Yang, P. Yan, M. Chen, C. Zhou, Y. Luo, Dynamic response of rock mass induced by the transient release of in-situ stress, 2012, *International Journal of Rock Mechanics & Mining Sciences*, vol. 53, no. 9, pp. 129-141.
7. N. Jiang, C. Zhou, Blasting vibration safety criterion for a tunnel liner structure, 2012, *Tunnelling & Underground Space Technology Incorporating Trenchless Technology Research*, vol. 32, no. 6, pp. 52-57.
8. D.P. Blair, Non-linear superposition models of blast vibration, 2008, *International Journal of Rock Mechanics & Mining Sciences*, vol. 45, no. 2, pp. 235-247.
9. H.R.M. Azizabadi, H. Mansouri, O. Fouché, Coupling of two methods, waveform superposition and numerical, to model blast vibration effect on slope stability in jointed rock masses, 2014, *Computers & Geotechnics*, vol. 61, no. 4, pp. 42-49.
10. H. Li, Y. Lv, Y. Liu, W. Qiao, S. Chen, Y. Yan, Influencing factor analysis of interference vibration reduction of millisecond blasting, 2012, *Disaster Advances*, vol. 5, no.4, pp. 494-501.
11. J.N. Brune, Tectonic stress and the spectra of seismic shear waves from earthquakes, 1970, *Journal of Geophysical Research*, vol. 75, no. 26, pp. 4997-5009.

12. M. Gong, H.J. Wu, X.D. Meng, Y.Q. Li, A precisely-controlled blasting method and vibration analysis for tunnel excavation under dense buildings, 2015, *Explosion & Shock Waves*, vol. 35, no. 3, pp. 350-358.
13. Z. Wu, N.E. Huang, A study of the characteristics of white noise using the empirical mode decomposition method, 2004, *Proceedings Mathematical Physical & Engineering Sciences*, vol. 460, no. 2046, pp. 1597-1611.
14. J.R. Yeh, J.S. Shieh, N.E. Huang, Complementary ensemble empirical mode decomposition: a novel noise enhanced data analysis method, 2010, *Advances in Adaptive Data Analysis*, vol. 2, no. 2, pp. 135 -156.